BULLETIN OF THE POLISH ACADEMY OF SCIENCES
TECHNICAL SCIENCES, Vol. 68, No. 6, 2020
DOI: 10.24425/bpasts.2020.135400



# Adaptation of models from determined chaos theory to short-term power forecasts for wind farms

T. POPŁAWSKI[1*], P. SZELĄG[1], and R. BARTNIK[2]

[1] Department of Electrical Engineering, Czestochowa University of Technology, Al. Armii Krajowej 17, 42-200 Czestochowa, Poland
[2] Department of Power Management, Opole University of Technology, ul. Ozimska 75, 45-370 Opole, Poland

**Abstract.** The paper proposes an adaptation of mathematical models derived from the theory of deterministic chaos to short-term power forecasts of wind turbines. The operation of wind power plants and the generated power depend mainly on the wind speed at a given location. It is a stochastic process dependent on many factors and very difficult to predict. Classical forecasting models are often unable to find the existing relationships between the factors influencing wind power output. Therefore, we decided to refer to fractal geometry. Two models based on self-similar processes (M-CO) and (M-COP) and the (M-HUR) model were built. The accuracy of these models was compared with other short-term forecasting models. The modified model of power curve adjusted to local conditions (M-PC) and Canonical Distribution of the Vector of Random Variables Model (CDVRM). Examples of applications confirm the valuable properties of the proposed approaches.

**Key words:** chaos theory, fractals, prognostic models, short-term forecasts, time series.

## 1. Introduction

Over the last decades, there has been a turnabout in the production of energy towards renewable energy sources. It has happened due to the gradual run-out of fossil fuel resources as well as growing activities to minimize the human impact on the natural environment and climate change. The consequence is the growing number of energy production facilities based on renewable resources. The greatest dynamics of growth has been recorded in the construction of new wind power plants. The World Wind Energy Association (WWEA) that has over 600 members from more than 100 countries reported that at the end of 2018 the wind power industry had 597 GW of installed power. The problem is that wind energy is the least predictable form of energy currently used for the needs of power supply systems. It depends strongly on many environmental conditions. The main factor is the wind speed, but other factors, such as the wind direction, atmospheric pressure, air temperature, terrain configuration, local terrain obstacles, height of a nacelle installation, etc. have a strong impact on the operation of wind power plants. Significant variations of possible power production in time enforce local power transmission operators to maintain power reserves in case of power production drop or even cut due to low wind speeds.

To reduce the potential negative effects of increasing contribution of wind power to the total power production, the development of special forecasting tools dedicated specifically to the wind power industry has been initiated [1–3]. The developed methods can be divided into two groups representing a different approach to the problem. The first group is based on a statistical approach and uses historical data to find out relationships between the power generated by a wind power plant and the corresponding wind speed [4–8]. The second group represents a physical modeling approach and is based on using information on global and local geographic and atmospheric conditions to develop a model that gives the best solution [9–11]. Developers of physical models try to recreate physical conditions that affect power generation and use forecasting tools only during the final stage. It should be noted, however, that the above division is not strict. Over the years methods that use both approaches have been worked out as well as complex techniques based on many methods and several data sources, but the common goal is always to minimize the resulting forecast error [12–14].

In the initial period of development of forecasting models for wind power plants researchers concentrated on tools utilizing time series analysis. This research has yielded several methods based on autoregressive (AR), moving average (MA), autoregressive moving average (ARMA), or autoregressive integrated moving average (ARIMA) models [1, 6–8].

The next widely developed groups have been models based on artificial neural networks working as independent prediction tools or linked with other forecasting methods [11–14]. The developed models were configured in diverse ways, had different numbers of inputs and outputs, hidden layers, and neurons. They were tuned to make predictions for various time horizons [15–20]. Complementary to power production forecasting methods, tools for wind strength estimation for a given area have been developed. All this research was significant from an economic point of view because it supported making decisions on the location of individual wind power farms.

*e-mail: poptom@el.pcz.czest.pl

Manuscript submitted 2020-02-06, revised 2020-06-23, initially accepted for publication 2020-09-23, published in December 2020

Currently, the most developed and used technique for wind-generated power forecasting is combining various models and creating complex systems based on several independent data sources. One of such methods, applied in Denmark, used the weather forecast delivered by the Danish Institute of Meteorology and based on the HIRLAM model as an input [21]. The forecast was processed by the WAsP software, the industry-standard for wind resource assessment, to take into account local conditions, and by the PARK application [22] to take into account the shadowing effect between wind turbines at the farm. After processing the data were passed to power production forecast models.

There also exist hybrid systems that combine several models and give reliable forecasts with smaller prediction error [13, 14, 23]. Other examples are methods that simultaneously use data delivered by a numerical weather forecast and a SCADA system [24] or a solution based on combining several weather forecasts. In general, one can observe a tendency to centralize prediction systems. The forecasts are created not for individual wind turbines or farms, but for groups of farms or even on the level of national power systems. These activities have led to the development of systems such as Predictor, WPPT, Sipreolico, LocalPred, Previento or eWind, whose forecasts cover areas of whole countries [13].

It is becoming increasingly difficult to classify systems developed nowadays. Nonetheless, in each of them one can identify the components presented in Fig. 1. A forecast system can utilize input data from one of the presented sources, their combination, or all available types of information. There exists also a vast diversity of models. The use of a single model is becoming occasional due to the high probability of a major forecast error. The most popular end effective solutions include several forecast tools to average and reduce prediction errors. The horizon of the produced forecast is determined by the two sources mentioned earlier. Systems based on a statistical approach and using data from SCADA systems generate short-term forecasts with satisfactory accuracy, but in general the longer the time horizon is, the less accurate prediction one can make. If a numerical weather forecast is used, its horizon determines the prediction horizon for the wind power plant operation.

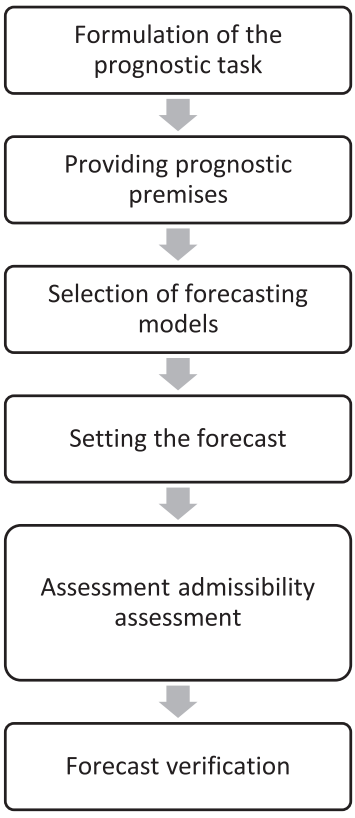


Fig. 1. Diagram of the stages of the construction process and tests of the forecasting models described in the article

Initial attempts to create forecasts for the needs of the wind power production industry date back to the turn of the the 1970s and 1980s, but rapid progress in the development of prediction methods and systems has been observed only over the recent 20 years. It is associated with the dynamic growth of the new installed wind power units and increasing participation of wind power in total power production. Therefore, despite all the previous work and progress in this field, researchers are still looking for new solutions that would improve the forecast accuracy. One of the promising directions of research that gives hope for a better description of the investigated phenomena is deterministic chaos.

In our initial research experiments we employed various forecast models based on autoregressive and moving average models and other econometric models, e.g. those implemented in the CDVRM application. Unfortunately, these attempts were labor-consuming and did not bring satisfactory results coinciding with the accuracy of well-known forecast models dedicated to wind power plants [1–3].

Currently, one of the new directions in the research of non-stationary time series that portends well for the future is the deterministic chaos theory [25–27]. Models that employ deterministic chaos and specific properties of fractal series create quite a new and separate group of forecast methods. Attempts of using fractal properties for long-term forecasting were described in [26], but they were more frequently used for short-term forecasting [25, 28, 29]. This paper is a continuation of the Authors' work on improving methods that use elements of fractal geometry. Fractal geometry is employed to build forecast models based directly on the self-similarity properties of time series or on the fractal measure. Two models based on self-similar processes are presented: (M-CO) and (M-COP) as well as the (M-HUR) model that uses relationships associated with a fractal dimension.

## 2. Fractal analysis and statistical processes

The fractal analysis is based on the idea of a fractal. There is no precise definition of a fractal, it is defined by its properties [30-32]. The most mentioned properties of fractals are:

- Nontrivial structure;
- Difficulty to describe a fractal using traditional geometry;
- Self-similarity in the exact, approximate, or stochastic sense;

- The Hausdorff dimension of a fractal exceeding its topological dimension;
- Relatively simple recursive definition;
- Natural (jagged, billowy, etc.) look.

The results presented in the paper are based on using the fractal properties described in the context of time series analysis, e.g. in [25–35], whose plots can be compared to a sea coastline. The greater is the magnification of a coastline, the more details are visible. This can also be applied to some time series. If they are observed over increasingly shorter time intervals, they may exhibit a very interesting property of a statistical self-similarity in different scales.

Performing the Dickey-Fuller tests for nonstationarity of the time series shown in Fig. 2 and inferring with 5% significance level, we obtained p-values much higher than 0.05 for a one-day waveform (p-value = 0.5651) and for a one-week waveform (p-value = 0.3201). Only for a four-week waveform, p-value = 0.0002696 is less than the test level, which may prove the stationarity of this time series. For better confidence, we also performed the Kwiatkowski–Phillips–Schmidt–Shin (KPSS) tests for the presented time series. In this case, inferring with 5% significance level as before, all the test statistics, with or without trend, turned out to be higher than the critical value, which shows the nonstationarity of all three-time series.

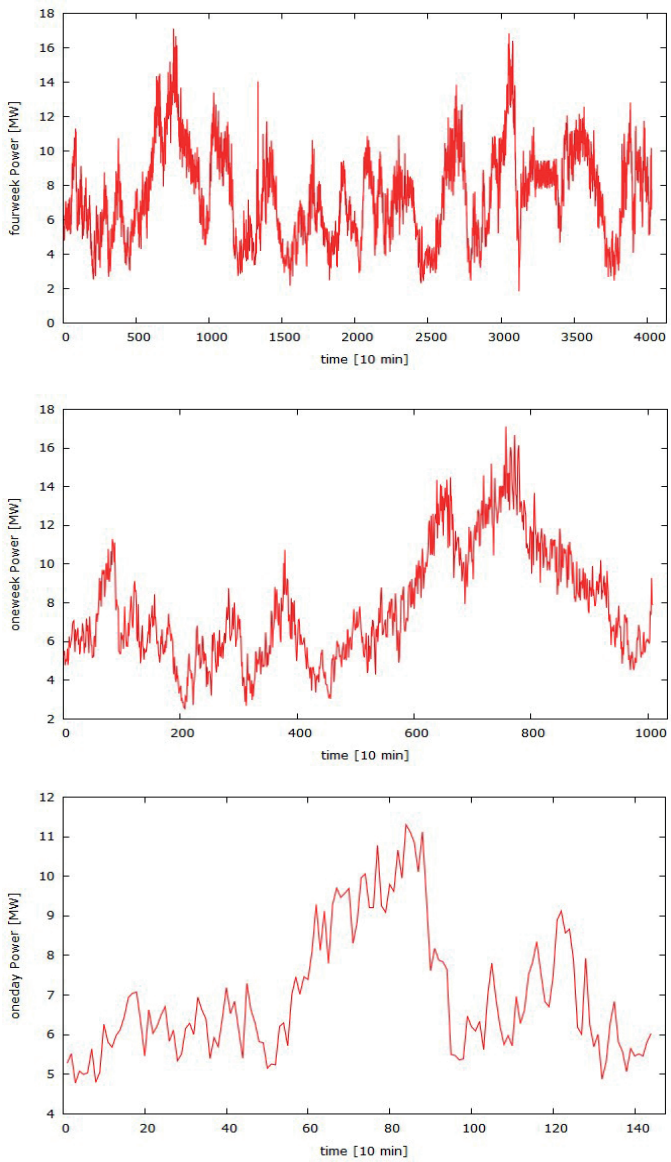


Fig. 2. Time series of electric power produced by wind farm F3 in different time scales: four weeks, one week and one day, respectively

Time series possessing such a property are called fractal series. It is worth adding that self-similar fractal time series exhibit long-term correlations. One of the important analysis tools of a fractal time series is determining its fractal dimension, which is a measure of how much the series plot line is jagged.

The fractal dimension can be evaluated graphically starting from the definition of the compass dimension or the box dimension, but this method is time-consuming. Instead, the Hurst exponent is used in the paper to determine the fractal dimension of a time series. The relationship between the fractal dimension and the Hurst exponent is [31]:

$$D = 2\mathrm{H}, \tag{1}$$

where: $D$ – fractal dimension; $H$ – Hurst exponent.

Using Eq. (1) it is possible to determine the fractal dimension of a time series from its Hurst exponent. It is useful in a time series analysis for distinguishing their statistical properties. Depending on the Hurst exponent value, a time series can be assigned to one the following three classes:

1. $0 < \mathrm{H} < 0.5$ – antipersistent series,
2. $\mathrm{H} = 0.5$ – random series, no correlations,
3. $0.5 < \mathrm{H} < 1$ – persistent series.

The statistical analysis and modeling with the use of the Hurst exponent or chaos theory was applied with positive results in financial management and capital markets [29, 32, 33] but also in other strictly technological [28] or medical and biological [36, 37] processes.

**2.1. Hurst model (M-HUR).** Based on Hurst's results, we assume that most natural time series processes are no random walks. Since there exist similarities between a time series of wind plant power production and share prices, e.g. on the Warsaw stock exchange, we decided to adopt the method of Hurst exponent evaluation used for a financial time series [28].

For a given time series $X_t$, the mean $m$ is calculated and removed from the series:

$$Y_t = X_t - m, \qquad t = 1, 2, \ldots, n. \tag{2}$$

Next, the zero-mean series $Y_t$ is cumulated:

$$Z_t = \sum_{i=1}^{t} Y_t, \qquad t = 1, 2, \ldots, n, \tag{3}$$

and the series $R_t$ of the maximum deviation of the cumulated series $Z_t$ until $t$ is calculated:

$$R_t = \max(Z_1, Z_2, \ldots, Z_t) - \min(Z_1, Z_2, \ldots, Z_t), \qquad t = 1, 2, \ldots, n. \tag{4}$$

The standard deviations of the original series $X_t$ until $t$ are calculated as:

$$S_t = \sqrt{\frac{1}{t}\sum_{i=1}^{t}(X_i - u)^2}, \quad t = 1, 2, \ldots, n, \tag{5}$$

where: $u$ – mean of the series $X_1$ to $X_t$.

The mean rescaled range for subsets:

$$[X_1, X_t], \ [X_{t+1}, X_{2t}] \ldots \left[X_{(m-1)(t+1)}, X_{mt}\right], \tag{6}$$

where: $m$ – rounding down to integer of the ratio $\frac{n}{t}$ is calculated as:

$$\left(\frac{R}{S}\right)_t = \frac{R_t}{S_t}, \qquad t = 1, 2, \ldots, n. \tag{7}$$

The mean rescaled range is a power function of time with Hurst exponent $H$, given as:

$$\left(\frac{R}{S}\right)_t = ct^H, \qquad t = 1, 2, \ldots, n, \tag{8}$$

where: $c$ – constant.

In the logarithmic scale formula (8) can be rewritten as:

$$\log\left(\frac{R}{S}\right)_t = \log c + H \log t. \tag{9}$$

The slope, i.e. Hurs exponent $H$, of the above linear function of the rescaled range $\log(R/S)_t$ versus $\log t$ can be determined using linear regression and the least squares method.

The top graph in Fig. 3 depicts an example time series of power generated by a single wind turbine, recorded at 10-minute sampling interval, and the top graph in Fig. 4 shows

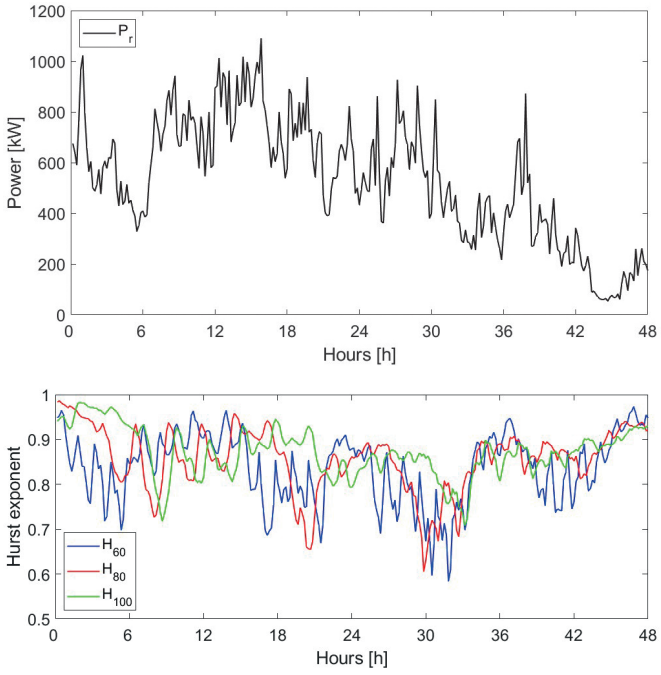


Fig. 3. Time series of power generated by wind turbine W5 (at 10-minute sampling interval) (top) and plots of the corresponding Hurst exponent calculated using 60, 80 and 100 samples (bottom)

the power generated by a whole wind power farm at 10- minute sampling interval. The bottom graphs in Figs. 3 and 4 show plots of the Hurst exponent calculated for the corresponding power time series using 60, 80 and 100 samples. The samples were chosen to check properties of the time series at a short time interval and, at the same time, provide a minimum number of samples necessary for the correct work of the Hurst exponent determination algorithm.

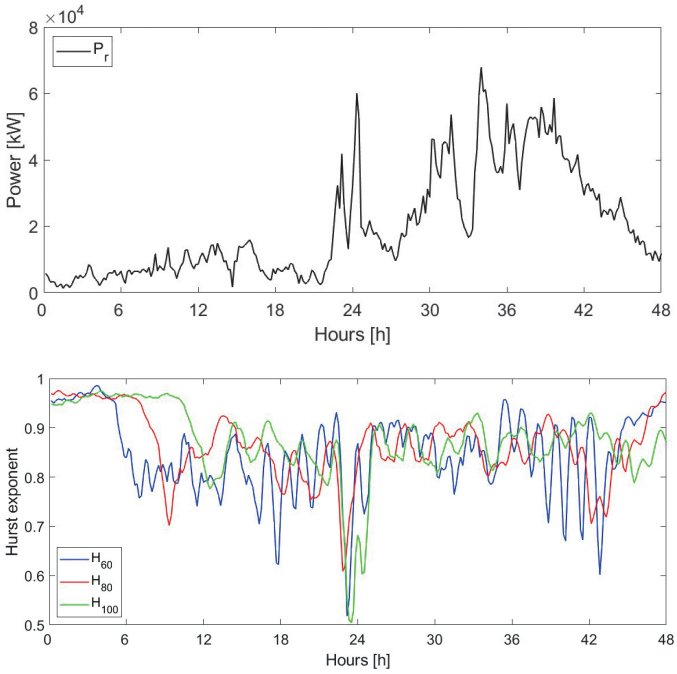


Fig. 4. Time series of power generated by wind power farm F3 (at 10-minute sampling interval) (top) and plots of the corresponding Hurst exponent calculated using 60, 80 and 100 samples (bottom)

The plots of the Hurst exponent depend on the length of the time interval over which the exponent was determined (i.e. the number of samples taken for calculation). It does not change the fact that the obtained range of the Hurst exponent allows us to claim that the power production plots represent persistent time series. Most of the time the Hurst exponent is above 0.8, which means that the process has a strong tendency to enhance its trend.

The Hurst exponent is also a measure of how much time the series plot is jagged. The greater is the Hurst exponent, the smoother is the process plot, and the time series gains deterministic properties. It was confirmed by an analysis carried out both for single wind turbines and for wind power farms. Data recorded at shorter time intervals exhibit much higher variation of generated power. It results from the fact that the factors affecting the instant power generated by wind turbines are mostly short-time disturbances (e.g. rapid wind gusts). Recording data at a greater sampling interval reduces the impact of such short-time disturbances.

It should be noted that a high value of the Hurst exponent not always indicates the persistency of the corresponding time series. According to [31, 32], there are two ways of explaining

a situation when the Hurst exponent significantly differs from 0.5: a given series exhibits the memory effect and each observation is correlated with the preceding ones or the conducted analysis is incorrect and the obtained exponent value does not prove that the corresponding process exhibits the memory effect. Fortunately, there is a method to verify the obtained results [31, 32]. After determining the Hurst exponent for a given sample series, the observations should be mixed so that their order in the new series is different from the original one. Then, the Hurst exponent is determined again for the mixed series. If the original series is independent, the exponent value should be the same, because the memory effect does not occur. If the Hurst exponent of the mixed series is much closer to 0.5, it indicates that the original series exhibits the memory effect, and the process structure was destroyed after mixing.

The evaluation of the Hurst exponent was accompanied by the verification of the statistical hypothesis about the correlations existing in the analyzed time series. Such correlations might reveal memory effects in processes that model the operation of wind turbines and power plants.

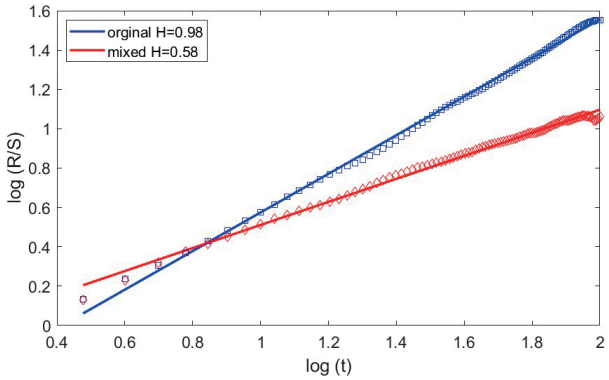


Fig. 5. Hurst exponent evaluated from a part of the time series (original and mixed) of power generated by wind turbine W5, recorded at 10-minute sampling interval

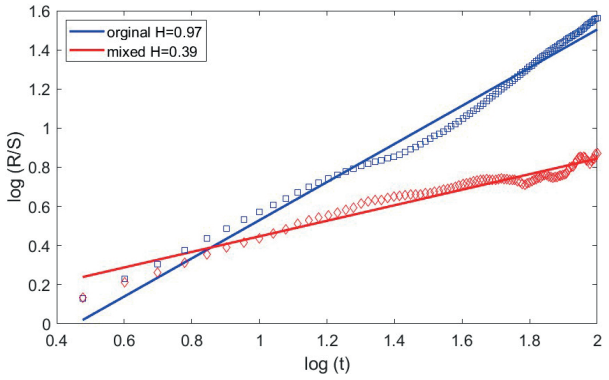


Fig. 6. Hurst exponent evaluated from a part of the time series (original and mixed) of power generated by wind power farm F3, recorded at 10-minute sampling interval

The example results of linear regression, calculated according to (9) for a single wind turbine and for a wind power plant and shown in Figs. 5 and 6, respectively, confirm observations from the research. In both cases, the Hurst exponent values determined from the original empirical data (slopes of blue linear regression fits) are greater than 0.5. The Hurst exponents determined for time series obtained after random mixing of the original data (slopes of red linear regression fits) are significantly smaller. The series after data mixing do not exhibit dependencies between successive observations and data correlations are significantly smaller. The presented results prove that the process memory occurs in the original time series.

Model building (M-HUR) has been implemented in the CDVRM prognostic tool. Assume that a given process is described with a random vector $\mathbf{X}$, for which the components $\mathbf{X}_i$ ($i = 1, 2, \ldots, m$) are correlated with each other. Transforming a vector $\mathbf{X}$ having components correlated to another vector $\mathbf{V}$ with uncorrelated components, which are linear functions of vector $\mathbf{X}$ components, may be performed using the method of canonical distribution. This method is described in detail in [25].

Generally, when using the CDVRM two possibilities may occur:

1. Only the realization of the first component $X_1$ is known, and all the remaining components $X_2, \ldots, X_{m-1}, X_m$ are forecasted.
2. The realizations of the $p$ components are known, then $(m-p)$ variables are forecasted.

In the described case, option 2 was used in the article. Variables $X_1, X_2$ up to $X_p$ in the forecast are considered as explanatory variables, components $X_{p+1}$ and further are endogenous variables.

The equation to determine a forecast for the $i$-th component (variable) is as follows:

$$\hat{Y}_i = \sum_{j=1}^{i-1} a_{i,j} V_j + \hat{V}_i + \bar{x}_i \,, \tag{10}$$

where: $a_{ij}$ – canonical distribution coefficients selected to ensure lack of correlations for variables $V_i$, $V_j$ – vector $V$ components after canonical distribution, $\hat{V}_i$ – components of the V vector drawn from the conditional cumulative distribution function (in (M-HUR) model wind speed), $\bar{x}_i$ – mean value of component $X_i$.

**2.2. Self-similar process model (M-CO).** Self-similar process models are adequate when there exists a strong correlation between the analyzed time series and/or autocorrelation in historical data of the quantity to forecast. Direct and strong influence of wind speed on the power generated by a wind power plant should find be reflected in the strong cross-correlation between the corresponding time series. In addition, the occurrence of autocorrelation was found out in time series representing the generated electric power. These observations were verified and confirmed by the analysis presented below.

The corresponding parts (series over the same time interval) of the time series representing the wind speed and the generated power were selected randomly from the available data. Each sample included 300 pairs of data points. The representative

results of statistical tests carried out for single wind turbines and for wind power farms are presented in Tables 1 and 2, respectively. The results reveal a strong correlation between the two-time series and justify the adoption of a model based on the strong correlation between processes for prediction in the field of wind power generation.

Table 1
Pearson correlation coefficient for selected parts of the time series of wind speed and generated power for three wind power farms. Source: own elaboration

| Farm number | Pearson correlation coefficient |
|---|---|
| 1 | 0.9476 |
| 2 | 0.9088 |
| 3 | 0.9767 |

Table 2
Pearson correlation coefficient for selected parts of the time series of wind speed and generated power for fifteen wind turbines. Source: own elaboration

| Turbine number | Pearson correlation coefficient |
|---|---|
| 1 | 0.9291 |
| 2 | 0.9186 |
| 3 | 0.9317 |
| 4 | 0.9734 |
| 5 | 0.9766 |
| 6 | 0.9498 |
| 7 | 0.9591 |
| 8 | 0.9686 |
| 9 | 0.9438 |
| 10 | 0.9271 |
| 11 | 0.9135 |
| 12 | 0.9264 |
| 13 | 0.9341 |
| 14 | 0.9211 |
| 15 | 0.9525 |

(M-CO) algorithm based on self-similar processes is defined by the following equation:

$$\hat{Y}_{t+1} = \hat{C}_{\frac{t}{t}} X_{t+1}\,, \tag{11}$$

where: $\hat{C}_{\frac{t}{t}}$ – self-similarity coefficient calculated as:

$$\hat{C}_{\frac{t}{t}} = \frac{\sum_{i=t-k}^{t} Y_i X_i}{\sum_{i=t-k}^{t} X_i^2}\,. \tag{12}$$

In the context of wind power generation forecasting, a slight modification of denotation was introduced in this paper and an estimate of the wind speed is used in Equation (13) because its actual value at time $t+1$ is unknown. The relationship between the estimated wind speed and power is as follows:

$$\hat{P}_{t+1} = \hat{C}_{\frac{t}{t}} \hat{v}_{t+1}\,, \tag{13}$$

where: $\hat{v}_{t+1}$ – predicted wind speed, $\hat{C}_{\frac{t}{t}}$ – self-similarity coefficient calculated as:

$$\hat{C}_{\frac{t}{t}} = \frac{\sum_{i=t-k}^{t} P_i v_i}{\sum_{i=t-k}^{t} v_i^2}\,. \tag{14}$$

Numerical experiments showed that by using logarithms of the data, fast changes of coefficient $\hat{C}_{\frac{t}{t}}$ are significantly reduced. Therefore, the final equations of the (M-CO) forecast model take the following form:

$$\hat{P}_{t+1} = \exp\left(\hat{C}_{\frac{t}{t}} \ln \hat{v}_{t+1}\right), \tag{15}$$

$$\hat{C}_{\frac{t}{t}} = \frac{\sum_{i=t-k}^{t} \ln P_i \ln v_i}{\sum_{i=t-k}^{t} (\ln v_i)^2}\,. \tag{16}$$

**2.3. Modified self-similar process model (M-COP).** For the correct work of (M-CO) algorithm, it is necessary that the coefficient $\mathrm{Ct}_{/t}$ changes slowly and its sign does not change. It can be ensured when the basic model (13) is modified to the following form:

$$\hat{P}_{t+1} = \hat{C}_{(\frac{t}{t})COP} \hat{v}_{t+1}\,, \tag{17}$$

where: $\hat{v}_{t+1}$ – predicted wind speed, $\hat{C}_{(\frac{t}{t})COP}$ – corrected self-similarity coefficient calculated as:

$$\hat{C}_{(\frac{t}{t})COP} = \frac{\sum_{i=t-k}^{t} U_i W_i}{\sum_{i=t-k}^{t} W_i^2}\,, \tag{18}$$

where the new variables $U_t$ and $W_t$ are simply two-point means of the original data:

$$\mathrm{U}_t = 0.5\,(P_t + P_{t-1})\,, \tag{19}$$

$$\mathrm{W}_t = 0.5\,(v_t + v_{t-1})\,. \tag{20}$$

After applying logarithms, the modified (M-CO) forecast model takes the following form:

$$\hat{P}_{t+1} = \exp\left(\hat{C}_{(\frac{t}{t})COP} \ln \hat{v}_{t+1}\right), \tag{21}$$

where: $\hat{v}_{t+1}$ – predicted wind speed, $\hat{C}_{(\frac{t}{t})COP}$ – corrected self-similarity coefficient calculated from formula (18), where the

logarithmic variables:

$$U_t = 0.5\,(\ln P_t + \ln P_{t-1})\,, \tag{22}$$

$$W_t = 0.5\,(\ln v_t + \ln v_{t-1})\,. \tag{23}$$

Both models described by Equations (17) and (21) have been comprehensively tested for the accuracy of forecasts. These tests were carried out on the same statistical data and for the same forecast wind speed. However, due to the differences in their equations, they might produce, in general, different results. Therefore, further research focused on the model described by Equation (21) and all the results presented in the article relate to this model. By using several different basic models, one can develop more complex hybrid forecast methods and create models that are adequate to the local operating conditions of wind power plants.

## 3. Verification of the presented models

The three presented forecast models were verified using 105120 real world data points recorded over two years. Several hundred forecasts were calculated, from which only a few representative examples are presented in the paper. The forecast models were tuned using 120-hour data sequences and their prediction accuracy was verified using 480-hour data sequences.

An (M-PC) model created based on a power curve matched to local conditions was used as a reference model. The power curve was created using historical data for better representation of the actual work of a wind power plant. Next, the reference model was used to obtain the reference forecasts.

**3.1. Model input data.** The research was carried out using data from three wind farms of rated power 90MW, 50MW and 30MW. Detailed data were obtained from the 30MW farm, made up of fifteen 2MW wind turbines. For practical reasons, the research focused mainly on 3-hour and 24-hour forecasts. It was due to the binding legal regulations in Poland. The operator of the power distribution system allows for creating schedule units for wind-based power sources. Making one day schedules requires 24-hour forecasts. Moreover, the central power balancing system allows for correction of the power scheduled to be delivered to the grid from wind-based sources no later than 2 hours before the power generation. This requires 3-hour forecasts for the purposes of potential schedule corrections.

In Table 3 above, there are presented classic statistical measures determined for the tested farms and individual power plants. In the conducted research we tried to find the answer to the following question: Can the same tested models be used for both wind farms and individual power plants? The coefficient of variation, which compares the variability of features in two different populations, was used for this. In the case of wind farms, the value of this coefficient ranged from 35% to 45%, and in the case of individual wind turbines its value ranged from 25% to 35% (less than 45%). It follows from the fact that both the tested wind farms and individual wind turbines belong to the same range of the average wind variability. The same applies to

Table 3
Statistical measures for wind power farm F3 and wind turbine W5
Source: self-study

| Statistical measure | F3 | | W5 | |
|---|---|---|---|---|
| | Wind speed [m/s] | Power [kW] | Wind speed [m/s] | Power [kW] |
| Mean | 7.24 | 26715.00 | 7.29 | 681.22 |
| Median | 6.90 | 20900.00 | 7.30 | 575.00 |
| Minimum | 1.70 | 0.00 | 4.00 | 42.00 |
| Maximum | 18.70 | 85600.00 | 12.80 | 2059.00 |
| Standard deviation | 2.92 | 21721.00 | 1.74 | 463.25 |
| Coefficient of variation | 0.40 | 0.81 | 0.24 | 0.68 |
| Skewness | 0.72 | 0.87 | 0.16 | 0.94 |
| Kurtosis | 0.27 | -0.15 | -0.44 | 0.24 |
| 5%Percentile | 3.20 | 2100.00 | 4.40 | 124.00 |
| 95%Percentile | 12.80 | 72800.00 | 10.20 | 1625.70 |
| Q3Q11Range | 4.00 | 31600.00 | 2.40 | 602.50 |

the production of energy by a wind farm and by a single wind turbine. Both belong to the same range of the strong power variability (less than 100%). Comparison of the median and average values in the investigated processes showed that more extreme cases occur in the case of wind farms. The determined kurtosis coefficients testify to the difference in the flattening of distributions for farms and individual power plants.

The historical data encompassed actual wind speed data. To carry out the power prediction procedure in practice, the wind speed, which is the input data to the prediction models, also undergoes prediction. Due to difficulties with access to metrological forecasts including wind speed and concerning the same area and the same period, which could be used as an input to forecast models, the available actual wind speed data were disturbed to obtain the required "predicted" time series. The maximum relative value of the disturbance was $\pm 10\%$ (the range is 20%). This trick allowed us to simulate typical situations with the disturbance level corresponding to the wind speed prediction error. In [38], which deals with modelling accuracy of selected metrological parameters, two metrological models are compared: the Atmosphere Mesoscale Prediction System (COAMPS) and the integrated wave-current model (WAM-POM). In the case of the wind speed, they show that the differences between the models, in terms of the mean square error, are less than 2 meters per second, and the coefficients of variation are greater than 35%. There are high correlation coefficients between the models, from 0.7 to 0.84, which indicates that both (commonly used) models can provide good forecasts. Meteograms for the COAMPS model are generated in the nodes of the computation grid spaced 39 km apart. In addition, the UCM uses the UM model, which is based on the grid nodes spaced 4 km apart. The area, in which the wind farms described in this paper are located, is approximately of the same size. Therefore, it is reasonable to assume that the wind speed forecasts prepared for the models have enough error margin.

The input data were investigated from the point of view of their statistical measures. The list of these measures, calculated for one wind farm and one wind turbine, is presented in Table 3.

**3.2. Software tools used in research.** The main tool used for numerical implementation of the presented forecast models was Matlab (ver. 2016b). In the case of three models (M-PC, M-CO, M-COP), Matlab was the only programming environment used to compute forecasts and present results. The first stage was preparation of necessary time series of data, which included the generated power, actual wind speed and simulated wind speed. Functionally separate parts of the algorithms for three models were coded as Matlab functions. These functions were called by Matlab scripts that executed successive stages of the forecasting, starting from reading the data series, next computing the predicted power, comparing the predictions with actual data, and finally storing the results.

In the case of the (M-HUR) model, Matlab was used to evaluate the Hurst exponents for a given time series. Next, the corresponding value of the exponent was evaluated for each measurement point using data about power produced by the plants. The results of these computations, together with the database created earlier, were transferred to the MRK (*canonical distribution model*) software, where the block processing option was selected to compute forecasts more than one-step ahead. Depending on the selected option value the prediction horizon changed from three to twenty-four hours. An example single forecast is shown in Fig. 7.

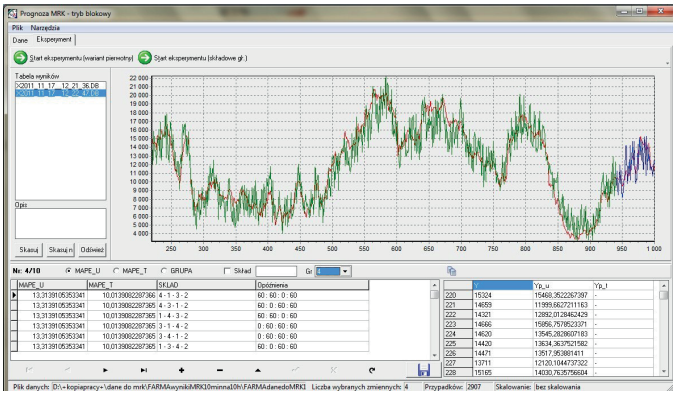

Fig. 7. Main window of MRK application that uses the canonical distribution of random variable vector for forecasting

**3.3. Forecast results.** In the case of wind generated power, the traditional assessment of prediction quality does not fully reflect the practical usefulness of forecasts due to the specific character of wind power plants operation.

The forecasting performance of the considered models was compared by calculating the NMAPE (Nominal Mean Absolute Percentage Error) [19, 28, 39] errors defined as:

$$\mathrm{NMAPE} = \sum_{i=1}^{t} \left| \frac{P_i - \hat{P}_i}{P_N} \right|, \qquad t > n, \tag{24}$$

where: $P_i$ – actual power generated by a wind plant at $i$-th time instant,

$\hat{P}_i$ – predicted power for this plant at $i$-th time instant,

$P_N$ – rated power of this plant at the wind speed, for which the predicted power was calculated.

The use of normalized prediction errors in the forecasting of wind power generation is currently common, so many authors do not even emphasize this fact. However, in the article error values determined in the classical way (MAPE) are also presented (Figs. 9, 11, 13 and 15).

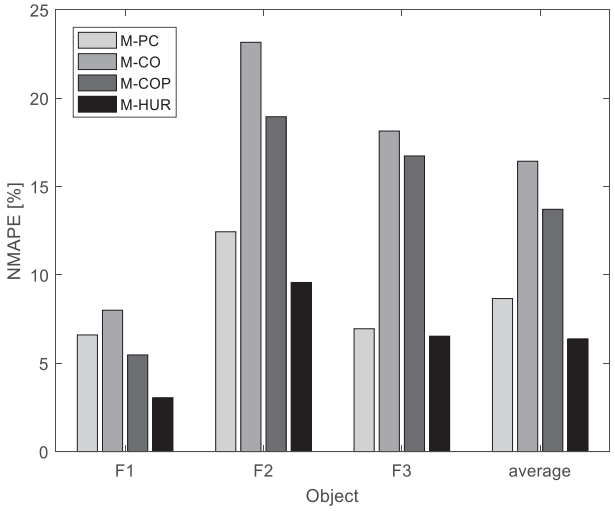


Fig. 8. Comparison of forecasting performance of the considered prediction models. The bars show NMAPE errors obtained for three wind farms F1–F3 and the average error for 3-hour ahead prediction; (M-PC) is the reference model

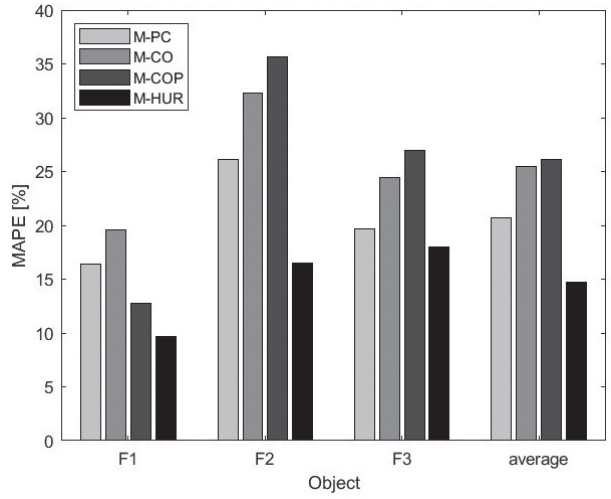


Fig. 9. Comparison of forecasting performance of the considered prediction models. The bars show MAPE errors obtained for three wind farms F1–F3 and the average error for 3-hour ahead prediction; (M-PC) is the reference model

Figure 8 presents the NMAPE errors of the considered forecast models, obtained for 3-hour ahead prediction using time

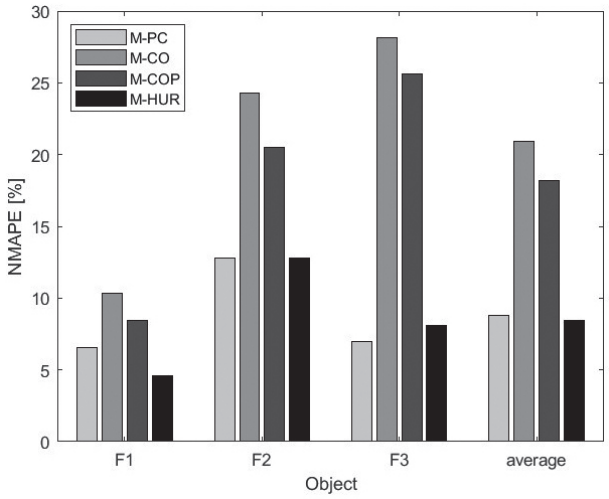


Fig. 10. Comparison of forecasting performance of the considered prediction models. The bars show NMAPE errors obtained for three wind farms F1–F3 and the average error for 24-hour ahead prediction; (M-PC) is the reference model

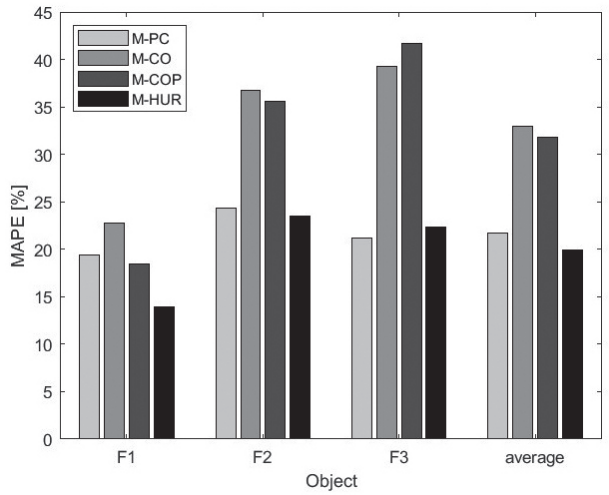


Fig. 11. Comparison of forecasting performance of the considered prediction models. The bars show MAPE errors obtained for three wind farms F1-F3 and the average error for 24-hour ahead prediction; (M-PC) is the reference model

series data, with 10-minute sampling interval, from three wind power farms. These results show that the two models, i.e. (M-CO) and (M-COP), give clearly worse predictions than the reference model (M-PC). On the other hand, the prediction performance of the Hurst model (M-HUR) is relatively best for all three wind farms. Figure 9 shows the MAPE prediction errors obtained for the same forecasts that are shown in Fig. 8. In Figs. 10 and 11 there are presented the NMAPE and MAPE errors obtained for 24-hour ahead prediction forecasts. Increasing the forecast time horizon produces in an increase in the error value. In addition, the MAPE error values are more than twice as large as the NMAPE error determined for the same forecast. This relationship is visible both for wind farms (Figs. 8–11) and individual wind power plants (Figs. 12–15).

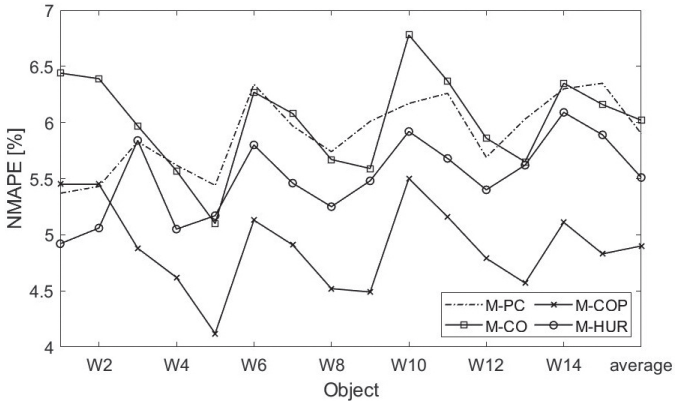


Fig. 12. Comparison of forecasting performance of the considered prediction models for fifteen wind turbines installed on the same wind farm. The points show NMAPE errors for wind turbines W1-W15 for 3-hour ahead prediction; (M-PC) is the reference model

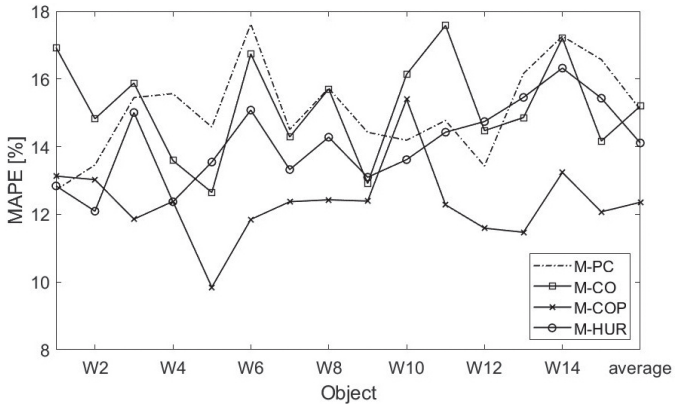


Fig. 13. Comparison of forecasting performance of the considered prediction models for fifteen wind turbines installed on the same wind farm. The points show MAPE errors for wind turbines W1-W15 for 3-hours ahead prediction; (M-PC) is the reference model

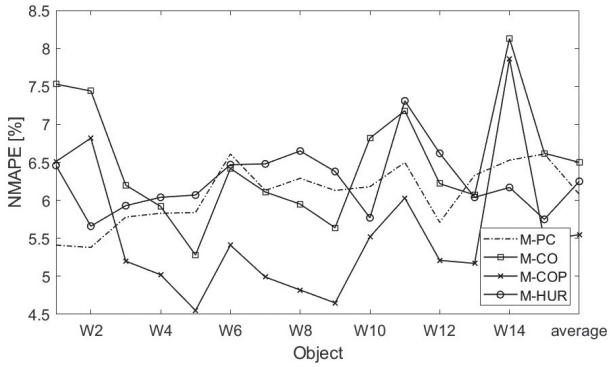


Fig. 14. Comparison of forecasting performance of the considered prediction models for fifteen wind turbines installed on the same wind farm. The points show NMAPE errors for wind turbines W1-W15 for 24-hour ahead prediction; (M-PC) is the reference model

The NMAPE errors of the models shown in Figs. 12 and 14 were calculated for time series from fifteen wind turbines installed on the same farm (for 3 and 24-hours ahead prediction

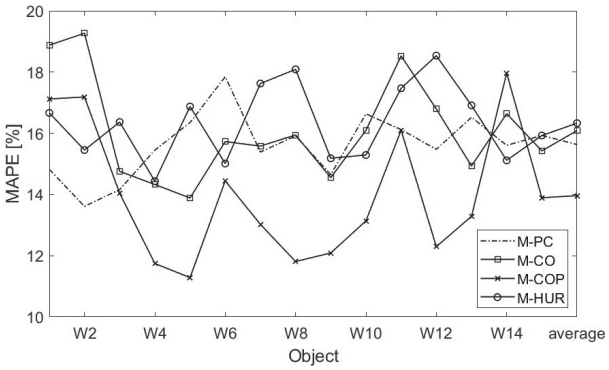


Fig. 15. Comparison of forecasting performance of the considered prediction models for fifteen wind turbines installed on the same wind farm. The points show MAPE errors for wind turbines W1-W15 for 24-hour ahead prediction; (M-PC) is the reference model

respectively and 10-minute sampling as before). In this case the (M-CO) model gave the worst predictions for 9 turbines (per 15), but its results are only slightly worse than for the reference model (M-PC). Clearly, whereas the best results were obtained for the (M-COP) model (for 13 turbines), with the performance of the Hurst model (M-HUR) this time somewhere in the middle.

The wind farm F3 consists of fifteen wind turbines. The levels of the NMAPE errors shown in Figs. 8 and 10 (for the whole wind farm) and in Figs. 12 and 14 (for the wind farm turbines) are different. It is due to different approaches to the evaluation of the forecast. The data for the wind farm F3 was aggregated using data from 15 individual wind turbines. The power generated by the wind turbines was summed up, whereas the wind speeds were averaged, and the average wind speed was disturbed as described in Section 3.1. The forecast was evaluated for the data prepared in this way. On the other hand, the forecast for each wind turbine was evaluated using individual turbine data, then the errors were determined for 15 turbine forecasts, and finally the mean error was calculated.

## 4. Conclusions

The results of the research presented and discussed in the paper allow us to formulate the following conclusions about the performance of the considered forecast models based on the deterministic chaos theory:

- Because of the method of determining the error, in each case the MAPE error value is greater than the NMAPE error value.
- Prediction error value is smaller for the forecasts with 3-hour ahead prediction than the forecasts with 24-hour ahead prediction.
- For the time series from the wind power farms, only the (M-HUR) model gave better predictions of the generated power than the reference (M-PC) model for 3-hour ahead prediction (Figs. 8, 9).
- For the time series from the wind power farms, the (M-HUR) model gave better predictions of the generated power than the reference (M-PC) model for farms F1 and F2; in the case of the farm F3 this value is slightly higher for 24-hour ahead prediction (Figs. 10, 11).
- For the time series from single wind turbines, the most accurate predictions were obtained for the (M-COP) model, but the (M-HUR) model also exhibited reasonable forecasting performance (Figs. 12–15).
- When power forecasts are required for a single wind turbine (M-COP) model should be preferred, its average NMAPE error for three wind farms was 6.38% for 3-hour ahead prediction and 8.47% for 24-hour ahead prediction; nonetheless, the prediction accuracy evaluated for other considered models does not disqualify any of the models.
- We recommend further work on the (M-HUR) model and on more complex hybrid models combining methods of artificial intelligence (fuzzy logic, artificial neural networks) that could make use of specific features of the (M-HUR) model to reveal memory in time series.

## References

[1] A. Augustyn and J. Kamiński, "A review of methods applied for wind power generation forecasting", *Polityka Energetyczna – Energy Policy Journal* 21(2), 139–150 (2018).

[2] H. Liu, Ch. Chen, X. Lv, X. Wu, and M. Liu, "Deterministic wind energy forecasting: A review of intelligent predictors and auxiliary methods", *Energ. Convers. Manage.* 195, 328–345 (2019).

[3] M. Lei, L. Shiyan, J. Chuanwen, L. Hongling, and Z. Yan, "A review on the forecasting of wind speed and generated power", *Renew. Sust. Energ. Rev*. 13, 915–920 (2009).

[4] E. Erdem and J. Shi, "ARMA based approaches for forecasting the tuple of wind speed and direction", *Appl. Energy* 88, 1405–1414 (2011).

[5] E. Cadenas and W. Rivera, "Wind speed forecasting in three different regions of Mexico, using a hybrid ARIMA-ANN model", *Renew. Energy* 35, 2732–2738 (2010).

[6] R.G. Kavasseri and K. Seetharaman, "Day-ahead wind speed forecasting using f-ARIMA models", *Renew. Energy* 34, 1388–1393 (2009).

[7] J. Torres, A. Garcia, M.D. Blas, and A.D. Francisco, "Forecast of hourly average wind speed with ARMA models in Navarre (Spain)", *Sol. Energy* 79, 65–77 (2005).

[8] A. Sfetsos, "A novel approach for the forecasting of mean hourly wind speed time series", *Renew. Energy* 27, 163–174 (2002).

[9] R. Blonbou, S. Monjoly, and J.F. Dorville, "An adaptive short-term prediction scheme for wind energy storage management", *Energ. Convers. Manage.* 52, 2412–2416 (2011).

[10] J. Catalao, H. Pousinho, and V. Mendes, "Short-term wind power forecasting in Portugal by neural networks and wavelet transform", *Renew. Energy* 36, 1245–1251 (2011).

[11] N.K. Paliwal, A.K. Singh, ang N.K. Singh, "Short-term optimal energy management in stand-alone microgrid with battery energy storage", *Arch. Elect. Eng*. 67(3), 499–513 (2018). doi: 10.24425/123659.

[12] G. Dudek, "Multilayer perceptron for short-term load forecasting: from global to local approach", *Neural Comput. Appl.* 32, 3695–3707 (2020). doi: 10.1007/s00521-019-04130-y.

[13] A.M. Foley, P.G. Leahy, A. Marvvuglia, and E.J. McKeog, "Current methods and advances in forecasting of wind power generation", *Renew. Energy* 37, 1–8 (2012).

[14] Z.S. Yang and J. Wang, "A combination forecasting approach applied in multistep wind speed forecasting based on a data processing strategy and an optimized artificial intelligence algorithm", *Appl. Energy* 230, 1108–1125 (2018).

[15] J, Wang, Y. Wang, and Y. Li, "A novel hybrid strategy using three-phase feature extraction and a weighted regularized extreme learning machine for multi-step ahead wind speed prediction", *Energies* 11(2), 321 (2018).

[16] I. Okumus and A. Dinler, "Current status of wind energy forecasting and a hybrid method for hourly predictions", *Energ. Conver.s Manage.* 123, 362–71 (2016).

[17] A. Zendehboudi, M. Baseer, and R. Saidur, "Application of support vector machine models for forecasting solar and wind energy resources: a review", *J. Clean Prod.* 199, 272–285 (2018).

[18] N. Amjady, F. Keynia, and H. Zareipour, "Short-term wind power forecasting using ridgelet neural network", *Elect. Pow. Syst. Res.* 81, 2099–2107 (2011).

[19] T. Barbounis and J. Theocharis, "A locally recurrent fuzzy neural network with application to the wind speed prediction using spatial correlation", *Neurocomputing* 70, 1525–1542 (2007).

[20] L. Thiaw, G. Sow, S. Fall, M. Kasse, E. Sylla, and S. Thioye, "A neural network based approach for wind resource and wind generators production assessment", *Appl. Energy* 87, 1744–1748 (2010).

[21] L. Landberg, "Short-term prediction of local wind conditions", *J. Wind. Eng. Ind. Aerod.* 89, 235–245 (2001).

[22] G. Giebel, L. Landberg, G. Kariniotakis, and R. Brownsword, "State-of-the-art on methods and software tools for short-term prediction of wind energy production", in *Proceedings of European wind energy conference*, Madryt, 2003.

[23] E. López, C. Valle, H. Allende, E. Gil, and H. Madsen, "Wind power forecasting based on echo state networks and long short-term memory", *Energies* 11(3), 526 (2018).

[24] A. Kusiak, H.-Y. Zheng, and Z. Song, "Wind Farm Power Prediction: A Data-Mining Approach", *Wind Energy* 12(3), 275–293 (2009).

[25] T. Poplawski, *Theory and Practice of Planning Development and Exploitation of Power Engineering Systems*, Technological University of Częstochowa, Częstochowa, 2013, [in Polish].

[26] T. Poplawski and D. Calus, "Adaptation of selected aspects of deterministic chaos for long-term forecasts of peak power demand for Poland", *Prz. Elektrotechniczny* R94 (12/2018), 79–85 (2018).

[27] I. Prigogine and I. Stengers, *Order out of Chaos*, University of Michigan, Bantam Books, 1984.

[28] T. Poplawski and P. Szelag, "Use the similarity of processes to predict the power output of wind turbines", *Energy Market* 92, 103–107 (2011) [in Polish].

[29] D. Grzech and G. Pamuła, "The local Hurst exponent of the financial time series in the vicinity of crashes on the Polish stock exchange market", *Physica A* 387, 4299–4308 (2008).

[30] B. Mandelbrot, *The Fractal geometry of nature*, W.H. Freeman & Co, 1982.

[31] H.O. Peitgen, H. Jurgens, and D. Saupe, *The borders of chaos, Fractals*, PWN Publishing House, 1997 [in Polish].

[32] E.E. Peters, *Chaos And Order In The Capital Markets – A New View Of Cycles, Prices, And Market Volatility*, Second Edition, John Wiley & Sons, New York, 1996.

[33] K. Domiono, "The use of the Hurst exponent to predict changes in trends on the Warsaw Stock Exchange", *Physica A* 390, 98–109 (2011).

[34] S.E. Kruger, O. Matos, J. Marcos, J. Mauricio, E.P.D. Moura, and A. Rebello, "Rescaled range analysis and fluctuation analysis study of cast irons ultrasonic backscattered signals", *Chaos Solitons Fractals* 19(1), 55–60 (2004).

[35] M. Gilmore, T.L. Rhodes, W.A. Peebles, and C.X. Yu, "Investigation of rescaled range analysis, the Hurst exponent, and long-time correlations in plasma turbulence", *Phys. Plasmas*. 9(4), 1312–1317 (2002).

[36] D.W. Qian, Y.F. Xi, and S.W. Tong, "Chaos synchronization of uncertain coronary artery systems through sliding mode", *Bull. Pol. Ac.: Tech*. 67(3), 456–462 (2019).

[37] Y. Li and X. Wang, "Improved dolphin swarm optimization algorithm based on information entropy", *Bull. Pol. Ac.: Tech* 67(4), 679–685 (2019).

[38] W. Cieslewicz and A. Dudtkowska, "The accuracy of some meteorological parameters modeling for the southern baltic sea area – a comparative study", Infrastructure and ecology of rural areas, 6/2011, PAN, 59–68, (2011) [in Polish].

[39] D.A. Swanson, J. Tayman, and T.M. Bryan, "MAPE-R: a rescaled measure of accuracy for cross-sectional subnational population forecasts", *J. Popul. Res.* 28, 225–243 (2011).